Received: 23 December 2021 | Revised: 4 February 2022 | Accepted: 8 March 2022
DOI: 10.1002/poc.4343

RESEARCH ARTICLE

Journal of Physical Organic Chemistry WILEY

Gas-phase experimental and computational studies of human hypoxanthine-guanine phosphoribosyltransferase substrates: Intrinsic properties and biological implications

Lanxin Zhang | Damon J. Hinz | George Sebastina Mary Kiruba | Xiao Ding | Jeehiun K. Lee

Department of Chemistry and Chemical Biology, Rutgers, The State University of New Jersey, New Brunswick, NJ, USA

Correspondence
Jeehiun K. Lee, Department of Chemistry and Chemical Biology, Rutgers, The State University of New Jersey, New Brunswick, NJ 08901, USA.
Email: jee.lee@rutgers.edu

Funding information
National Science Foundation

Abstract

The gas-phase acidity and proton affinity of nucleobases that are substrates for the enzyme human hypoxanthine-guanine phosphoribosyltransferase (HGPRT) have been examined using both theoretical and experimental methods. These thermochemical values have not heretofore been measured and provide experimental data to benchmark the computational results. HGPRT is important for human health and is also a key target for antiparasitic chemotherapy. We use our gas-phase results to lend insight into the HGPRT mechanism and also propose kinetic isotope studies that could potentially differentiate between possible mechanisms.

KEYWORDS

enzyme catalysis, gas-phase acidity, gas-phase proton affinity, kinetic isotope effects, organic mechanism

1 | INTRODUCTION

Hypoxanthine-guanine phosphoribosyltransferase (HGPRT) is an enzyme that is essential for purine salvage in both humans and parasites.[1] HGPRT catalyzes the formation of a glycosidic bond, via the transfer of a ribose phosphate moiety (5-phospho-α-D-ribose 1-diphosphate [PRPP]) to a purine nucleobase, to transform the purine nucleobase to a nucleoside monophosphate (Scheme 1, shown for hypoxanthine).[1–3]

In humans, a complete lack of HGPRT leads to Lesch–Nyhan syndrome, a condition characterized by severe neurological and behavioral abnormalities.[4] A partial HGPRT deficiency results in hyperuricemia, nephrolithiasis, and gouty arthritis.[5,6] HGPRT is also a target for antimalarial and antiparasitic treatments.[7–19] Mammalian cells can synthesize nucleic acids by the de novo pathway, as well as by the HGPRT "salvage" pathway. By contrast, protozoan parasites only have the salvage pathway for purines and the de novo pathway for pyrimidines. Thus, blocking the purine salvage pathway is a target for antimalarial design.[20] *Plasmodium falciparum* (*Pf*) is a parasite that is responsible for the most widespread and lethal malaria.[17] The analogous enzyme to human HGPRT is *Pf* HG(X)PRT.[16] *Pf* HG(X)PRT catalyzes the same reaction, of transferring the ribose to the nucleobase. It has a wider range of substrates, including xanthine (thus, the "X" in the enzyme name). The provenance of the wider substrate range of the *Pf* enzyme is not known.[21] Therefore, mechanistic studies to ascertain the similarities and differences between human HGPRT and *Pf* HG(X)PRT are important.[7,14,21–24]

Herein, we focus on the properties of human (Hu) HGPRT substrates. In prior work, we have found that the examination of properties in the gas phase, which provides the "ultimate" nonpolar environment, uncovers intrinsic, inherent reactivity that correlates to

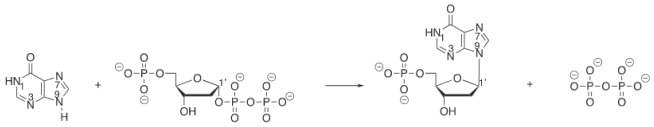

SCHEME 1 Reaction catalyzed by HGPRT

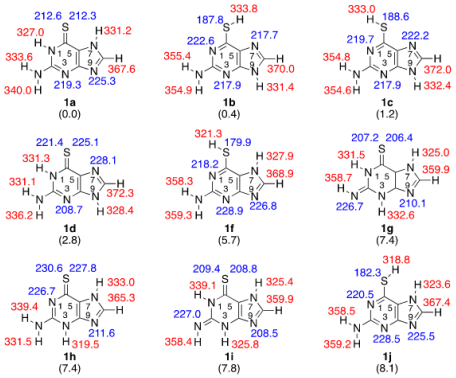

FIGURE 1 Calculated data for 6-thioguanine. Gas-phase acidities are in red; gas-phase proton affinities are in blue. Relative stabilities are in parentheses. Calculations were conducted at B3LYP/6-31+G(d); reported values are ΔH at 298 K, in kcal/mol

activity in other nonpolar media, including hydrophobic enzyme active sites.[25–36] In this paper, we calculate and measure the gas-phase acidities of a series of human HGPRT purine substrates not heretofore studied in vacuo. We also conduct energetics and KIE calculations; all these results are discussed in the context of the HGPRT mechanism.

2 | RESULTS

2.1 | 6-Thioguanine (6-Tg, 1)

2.1.1 | Calculations: Tautomers, acidity, and proton affinity

In our experience, calculations using B3LYP/6-31+G (d) generally yield accurate values for thermochemical properties of nucleobases, so we utilized this to calculate the relative tautomeric stabilities (relative enthalpies), acidities (ΔH_{acid}), and proton affinities (PAs) of 6-Tg.[25–36] 6-Tg (**1**) has many possible tautomeric structures; in Figure 1, the tautomers whose energies are within 10 kcal/mol of the most stable tautomer are shown. Data on the remaining tautomers are given in the supporting information. There are three tautomers within roughly 1 kcal/mol of the most stable tautomer. The most stable tautomer (N7H 6-Tg **1a**) is 0.4 kcal/mol more stable than the 6-thiol N9H tautomer **1b**. The next most stable tautomer is the rotamer (at the 6-thiol) of **1b** (**1c**), which is 1.2 kcal/mol less stable than **1a**. In terms of the thermochemical properties, the most acidic site of **1a** is calculated to be the N1–H (ΔH_{acid} = 327.0 kcal/mol). The most basic site of tautomer **1a** is the N9 (PA = 225.3 kcal/mol). Tautomer **1b** has a computed acidity of 331.4 kcal/mol (at N9–H) and a PA of 222.6 kcal/mol, at N1. The most acidic site of tautomer **1c** is the N9–H (ΔH_{acid} = 332.4 kcal/mol), whereas the most basic site is the N7 (PA = 222.2 kcal/mol).

2.1.2 | Experiments: Acidity and PA

The acidity of 6-Tg was assessed using Cooks' kinetic method (see Section 5 for details and the supporting information for data). The reference acids difluoroacetic

acid (ΔH_{acid} = 331.0 ± 2.2 kcal/mol), 3,5-bis(trifluoromethyl)phenol (ΔH_{acid} = 329.7 ± 2.1 kcal/mol), α,α,α-trifluoro-2,4-pentadione (ΔH_{acid} = 328.3 ± 2.9 kcal/mol), pentafluorophenol (ΔH_{acid} = 328.0 ± 2.2 kcal/mol), and 3,5-bis(trifluoromethyl)pyrazole (ΔH_{acid} = 324.6 ± 2.1 kcal/mol) were used, to yield a ΔH_{acid} for 6-Tg of 329 ± 3 kcal/mol.[37]

The PA of 6-Tg was also measured, using Cooks' kinetic method. The reference bases 4-picoline (PA = 226.4 ± 2.0 kcal/mol), 3-picoline (PA = 225.5 ± 2.0 kcal/mol), adenine (PA = 225.3 ± 2.0 kcal/mol), *tert*-amylamine (PA = 224.1 ± 2.0 kcal/mol), and cyclohexylamine (PA = 223.3 ± 2.0 kcal/mol) were used.[37] The measured PA (PA = Δ*H*) for 6-Tg is 225 ± 3 kcal/mol.

2.2 | 6-Mercaptopurine (6-Mp, 2)

2.2.1 | Calculations: Tautomers, acidity, and PA

In Figure 2, we show the four 6-Mp tautomers that are within 10 kcal/mol of the most stable structure (data on the remaining tautomers are given in the supporting information). The most stable tautomer (N7H **2a**) is 5.4 kcal/mol more stable than the N9H tautomer **2b**. The most acidic site of **2a** is calculated to be the N1–H (ΔH_{acid} = 327.0 kcal/mol). The most basic site of tautomer **2a** is the N9 (PA = 217.6 kcal/mol).

2.2.2 | Experiments: Acidity and PA

For Cooks' kinetic method acidity measurement, five reference acids were used: difluoroacetic acid (ΔH_{acid} = 331.0 ± 2.2 kcal/mol), 3,5-bis(trifluoromethyl) phenol (ΔH_{acid} = 329.7 ± 2.1 kcal/mol), α,α,α-trifluoro-2,4-pentadione (ΔH_{acid} = 328.3 ± 2.9 kcal/mol), pentafluorophenol (ΔH_{acid} = 328.0 ± 2.2 kcal/mol), and 3,5-bis(trifluoromethyl)pyrazole (ΔH_{acid} = 324.6 ± 2.1 kcal/mol), yielding an acidity (ΔH_{acid}) for 6-Mp of 328 ± 3 kcal/mol.[37]

The measurement of the PA of 6-Mp utilized the reference bases benzylamine (PA = 218.3 ± 2.0 kcal/mol), *m*-anisidine (PA = 218.2 ± 2.0 kcal/mol), *N*,*N*-dimethylacetamide (PA = 217.0 ± 2.0 kcal/mol), and *o*-anisidine (PA = 216.3 ± 2.0 kcal/mol). A PA of 218 ± 3 kcal/mol was obtained.[37]

2.3 | 8-Azaguanine (8-Ag, 3)

2.3.1 | Calculations: Tautomers, acidity, and PA

The 12 most stable 8-Ag tautomers are shown in Figure 3 (data on the remaining tautomers are given in the supporting information). The N9H structure **3a** is more stable than the N7H structure **3b** by 1.7 kcal/mol. The most acidic site of **3a** is at the exocyclic NH_2 (ΔH_{acid} = 327.9 kcal/mol). The most basic site is the N7 site, with a PA of 217.5 kcal/mol. The most acidic site of tautomer **3b** is calculated to be the N1–H (ΔH_{acid} = 326.0 kcal/mol). The most basic site of tautomer **3b** is the N9 (PA = 219.2 kcal/mol).

2.3.2 | Experiments: Acidity and PA

For the acidity measurement of 8-Ag, we used references pyruvic acid (ΔH_{acid} = 333.5 ± 2.9 kcal/mol), difluoroacetic acid (ΔH_{acid} = 331.0 ± 2.2 kcal/mol), 3,5-bis(trifluoromethyl)phenol (ΔH_{acid} = 329.7 ± 2.1 kcal/mol), and α,α,α-trifluoro-2,4-pentadione (ΔH_{acid} = 328.3 ± 2.9 kcal/mol), which yielded a ΔH_{acid} of 330 ± 4 kcal/mol.[37]

For the PA measurement of 8-Ag, four reference bases were used: *N*,*N*-diethylhydroxylamine (PA = 218.6 ± 2.0 kcal/mol), benzylamine (PA = 218.3 ± 2.0 kcal/mol), *m*-anisidine (PA = 218.3 ± 2.0 kcal/mol), and 3-bromo-pyridine (PA = 218.3 ± 2.0 kcal/mol). We measure a PA of 217 ± 3 kcal/mol.[37]

2.4 | Allopurinol (Apn, 4)

2.4.1 | Calculations: Tautomers, acidity, and PA

Apn (**4**) has three tautomers within 10 kcal/mol of the most stable tautomer (Figure 4, **4a**, **4b**, and **4c**; data on

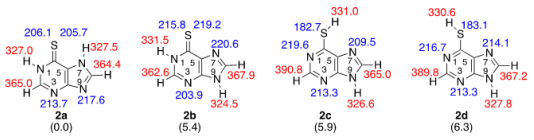

FIGURE 2 Calculated data for 6-mercaptopurine. Gas-phase acidities are in red; gas-phase proton affinities are in blue. Relative stabilities are in parentheses. Calculations were conducted at B3LYP/6-31+G (d); reported values are Δ*H* at 298 K, in kcal/mol

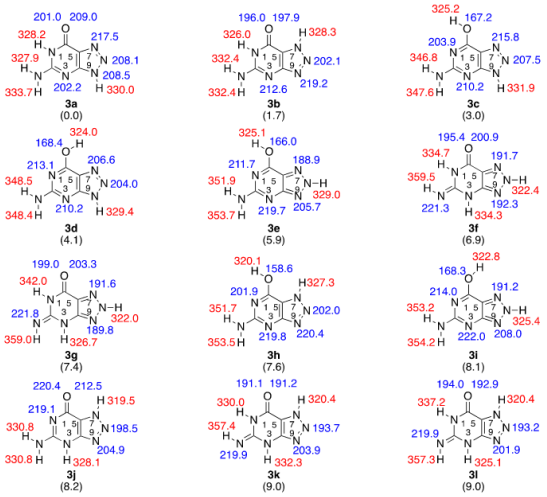

FIGURE 3 Calculated data for 8-azaguanine. Gas-phase acidities are in red; gas-phase proton affinities are in blue. Relative stabilities are in parentheses. Calculations were conducted at B3LYP/6-31+G(d); reported values are ΔH at 298 K, in kcal/mol[38]

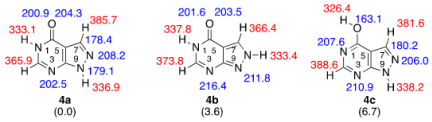

FIGURE 4 Calculated data for allopurinol. Gas-phase acidities are in red; gas-phase proton affinities are in blue. Relative stabilities are in parentheses. Calculations were conducted at B3LYP/6-31+G(d); reported values are ΔH at 298 K, in kcal/mol

remaining tautomers are in the supporting information). The most acidic site of **4a** is the N1–H, with a ΔH_{acid} of 333.1 kcal/mol. The most basic site of tautomer **4a** is the N8, with a PA of 208.2 kcal/mol.

2.4.2 | Experiments: Acidity and PA

We measured the acidity of Apn using Cooks' kinetic method. Seven reference acids were used: difluoroacetic acid ($\Delta H_{acid} = 331.0 \pm 2.2$ kcal/mol), α,α,α-trifluoro-*m*-toluic acid ($\Delta H_{acid} = 332.2 \pm 2.2$ kcal/mol), pyruvic acid ($\Delta H_{acid} = 333.5 \pm 2.9$ kcal/mol), 4-acetylbenzoic acid ($\Delta H_{acid} = 334.3 \pm 2.1$ kcal/mol), adenine ($\Delta H_{acid} = 335.3 \pm 2.2$ kcal/mol), 3-fluorobenzoic acid ($\Delta H_{acid} = 336.1 \pm 2.1$ kcal/mol), and 4,4,4-trifluorobutyric acid ($\Delta H_{acid} = 336.5 \pm 2.9$ kcal/mol), yielding a ΔH_{acid} of 335 ± 3 kcal/mol.[37]

Unlike the other purines that we studied, Apn is volatile enough to be vaporized from our solids probe, in our FTMS. We therefore also measured the acidity of Apn (**4**) using acidity bracketing (Table 1; see also Section 5 for details). Deprotonated 4,4,4-trifluorobutyric acid ($\Delta H_{acid} = 336.5 \pm 2.9$ kcal/mol) deprotonates Apn ("+" in the third column); the opposite reaction of the conjugate base of Apn with 4,4,4-trifluorobutyric acid also occurs ("+" in the fourth column). We therefore bracket the ΔH_{acid} of Apn as 337 ± 4 kcal/mol.

For PA, Cooks' kinetic method experiment had technical difficulties in producing the dimer, but we were able to measure the PA by bracketing, shown in Table 2. The results are somewhat surprising, on which we will elaborate in Section 3.

TABLE 1 Acidity bracketing of allopurinol (**4**)

Reference acid	ΔH_{acid} (kcal/mol)[a]	Proton transfer[b]	
		Deprotonated reference to substrate	Deprotonated substrate to reference
Difluoroacetic acid	331.0 ± 2.2	−	+
Pyruvic acid	333.5 ± 2.9	−	+
Malononitrile	335.8 ± 2.1	−	+
4,4,4-Trifluorobutyric acid	336.5 ± 2.9	+	+
Trifluoro-*m*-cresol	339.2 ± 2.1	+	−
Ethoxyacetic acid	342.0 ± 2.2	+	−
Acetylacetone	343.8 ± 2.1	+	−

[a]Linstrom and Mallard.[37]
[b]"+" indicates the occurrence of proton transfer, and "−" indicates the absence of proton transfer.

TABLE 2 Proton affinity bracketing of allopurinol (**4**)

Reference base	PA (kcal/mol)[a]	Proton transfer[b]	
		Protonated reference to substrate	Protonated substrate to reference
Diethyl sulfide	204.8 ± 2.0	+	−
Acetylacetone	208.8 ± 2.0	+	−
Pyrrole	209.2 ± 2.0	+	−
2′,4′-Dimethylacetophenone	210.9 ± 2.0	+	+
Pyrimidine	211.7 ± 2.0	+	+
o-Toluidine	212.9 ± 2.0	+	+
2-Chloropyridine	215.3 ± 2.0	+	+
N,*N*-Dimethylacetamide	217.0 ± 2.0	−	+
n-Propylamine	219.4 ± 2.0	−	+

[a]Linstrom and Mallard.[37]
[b]"+" indicates the occurrence of proton transfer, and "−" indicates the absence of proton transfer.

3 | DISCUSSION

3.1 | Calculated versus experimental values

The calculated acidity and PA values for the human HGPRT substrates are summarized in Table 3. As we noted earlier, in our experience, B3LYP/6-31+G(d) yields accurate values for thermochemical properties of nucleobases.[25–36] For the purines studied herein, the calculated and experimental values in Table 3 are in agreement, within the experimental error, indicating that B3LYP/6-31+G(d) appears to provide fairly accurate predictions for the thermochemical values. One exception is Apn PA, which we will discuss later in this section.

Although the computed and experimental acidity and PA values are in agreement, supporting the accuracy of B3LYP/6-31+G(d) for these thermochemical properties, we were still concerned about the relative tautomer

TABLE 3 Calculated (B3LYP/6-31+G(d); 298 K) and experimental data for purines

Substrate	Calculated value	Experimental value[b]
ΔH_{acid}[a]		
6-Thioguanine (**1**)	327.0	329
6-Mercaptopurine (**2**)	327.0	328
8-Azaguanine (**3**)	327.9	330
Allopurinol (**4**)	333.1	335 (337)
PA[a]		
6-Thioguanine (**1**)	225.3	225
6-Mercaptopurine (**2**)	217.6	218
8-Azaguanine (**3**)	217.5	217
Allopurinol (**4**)	208.2	(211–215)

[a]ΔH_{acid} and PA values are in kcal/mol.
[b]First listed experimental value is from Cooks' kinetic method; bracketing value, if available, is in parentheses. Error is ±3–4 kcal/mol.

enthalpies, particularly for 6-Tg, where **1a** and **1b** are so close in energy. To address this, we calculated the relative enthalpies of the four most stable tautomers of 6-Tg (**1**), 6-Mp (**2**), 8-Ag (**3**), and the three most stable tautomers of Apn (because Apn has fewer low-energy tautomers, **4**), using M06-2X/6-311++G(2d,p), B3LYP/D3(BJ)/6-311++G(2d,p), ωb97X-D/6-311++G(2d,p), and DLPNO-CCSD(T)/aug-cc-pVTZ//M06-2X/6-311++G(2d,p). These results are summarized in the supporting information. For all but 6-Tg, the most stable tautomer is consistent with that calculated at B3LYP/6-31+G(d). For 6-Tg, regardless of the method/level, structures **1a**, **1b**, and **1c** are the most stable; all have enthalpies within roughly 1 kcal/mol. At B3LYP/6-31+G(d), **1a** is more stable than **1b** by 0.4 kcal/mol. With M06-2X/6-311++G(2d,p), B3LYP/D3(BJ)/6-311++G(2d,p), and ωb97X-D/6-311++G(2d,p), structure **1b** is more stable, by 0.3, 0.2, and 0.7 kcal/mol, respectively. We also additionally calculated **1a** and **1b** at DPLNO-CCSD(T)/aug-cc-pVTZ//M06-2X/6-311++G(2d,p); at this level, **1a** is more stable than **1b**, by 1.2 kcal/mol. We can therefore only conclude that **1a** and **1b** are quite close in energy, with **1c** being a little less stable.

Because of these proximal computed ΔH values, under our experimental conditions, we may have one, two, or all three of these tautomers of 6-Tg present. Because the calculated acidities of the three most stable tautomers **1a**, **1b**, and **1c** are 327.0, 331.4, and 332.4 kcal/mol, respectively, and the measured acidity of 329 kcal/mol has a ±3 kcal/mol error bar, we cannot discount the possibility of more than one tautomer being present. The experimental PA is 225 ± 3 kcal/mol, whereas the computed PAs are 225.3, 222.6, and 222.2 kcal/mol for tautomers **1a**, **1b**, and **1c**, respectively. Again, the experimental error precludes knowing conclusively which tautomer(s) may be present. We also calculated the acidity and PA values using M06-2X/6-311++G(2d,p), and these values are consistent with the B3LYP/6-31+G(d) values, thus supporting our conclusion that we may have one or a mixture of tautomers **1a**, **1b**, and **1c**, under our experimental conditions.

8-Ag is also calculated to have two structures that are energetically within 2 kcal/mol of each other, **3a** and **3b**. The calculated acidities and PAs, like with 6-Tg, are too close to be used to conclude whether one or a mixture of tautomers is present.

We return now to Apn. We measured the PA of Apn using a bracketing method, in our FTMS. The bracketing result for Apn is of interest, as it yields a wide range, where proton transfer occurs in both directions (PAs from 210.9 to 215.3 kcal/mol [2′,4′-dimethylacetophenone, pyrimidine, *o*-toluidine, and 2-chloropyridine], Table 2).

In a PA bracketing experiment, the reaction of the compound whose PA is unknown (in this case, Apn) and a protonated reference base is examined. If proton transfer occurs, this is indicated by a "+" (third column, Table 2). If proton transfer does not occur, then this is indicated by a "−". Therefore, for the reaction of Apn and protonated diethyl sulfide, proton transfer is observed; thus, the first entry, third column, shows a "+". This indicates that Apn is more basic than diethyl disulfide. The reaction in the "opposite" or "reverse" direction is also studied: protonated Apn reacting with diethyl sulfide. For this reaction, we did not see proton transfer; thus, there is a "−" in the last column, first entry of Table 2. This is also consistent with Apn being more basic than diethyl sulfide. We therefore conclude that Apn has a PA value higher than that of diethyl sulfide (204.8 kcal/mol).

Sometimes, when the reference base and the substrate have similar PAs, the table may show a "+" for the reaction in both directions. In Table 2, this is the case for the reference base 2′,4′-dimethylacetophenone: There is a "+" entry in both the third and fourth columns. This would indicate that Apn must have a PA close to that of 2′,4′-dimethylacetophenone, around 210.9 kcal/mol. However, what is surprising is that this "+, +" in the third and fourth columns occurs for several bases. The reaction was found to occur in both directions (protonated reference base to Apn and protonated Apn to reference base) for reference bases with PAs from 2′,4′-dimethylacetophenone (210.9 kcal/mol) to 2-chloropyridine (215.3 kcal/mol).

Apn has two tautomers that are somewhat close in energy: The N9H tautomer **4a** and the N8H tautomer **4b** are calculated to be within 3.6 kcal/mol, regardless of computational method or level (Figure 4 and the supporting information). Interestingly, these two tautomers have quite dissimilar PAs: Although **4a** is calculated to have a PA of 208.2 kcal/mol, **4b** has a computed PA of 216.4 kcal/mol. (We also calculated these values at M06-2X/6-311++G(2d,p), and they are consistent with the B3LYP/6-31+G(d) values.) We suspect that both tautomers are present, resulting in the wide bracketed PA range.[33]

If only **4a** were present, we would expect a bracketed PA of around 208 kcal/mol, based on the calculations (Figure 4 and Table 3). The bracketing table would have a clean "crossover" point near pyrrole, as shown in Table 4.

If only **4b** were present, one would expect a "crossover" point close to the PA of the most basic site of **4b**, which is calculated to be 216.4 kcal/mol (Figure 4). If this were the case, the data shown in the bracketing table would show a change from "+, −" to "−, +" around

TABLE 4 *Hypothetical* bracketing table if only **4a** were present

Reference base	PA (kcal/mol)[a]	Proton transfer[b]	
		Protonated reference to substrate	Protonated substrate to reference
Diethyl sulfide	204.8 ± 2.0	+	−
Acetylacetone	208.8 ± 2.0	+	−
Pyrrole	209.2 ± 2.0	−	+
2′,4′-Dimethylacetophenone	210.9 ± 2.0	−	+
Pyrimidine	211.7 ± 2.0	−	+
o-Toluidine	212.9 ± 2.0	−	+
2-Chloropyridine	215.3 ± 2.0	−	+
N,*N*-Dimethylacetamide	217.0 ± 2.0	−	+
n-Propylamine	219.4 ± 2.0	−	+

[a]Linstrom and Mallard.[37]
[b]"+" indicates the occurrence of proton transfer, and "−" indicates the absence of proton transfer.

2-chloropyridine or *N*,*N*-dimethylacetamide. Instead, there is no clean crossover point but a range in which the proton transfer occurs in both directions (Table 2). We suspect that the reason for this is the presence of both tautomers **4a** and **4b**.

For the reaction of protonated Apn with the reference bases, if both tautomers are present, then the protonated Apn will be a mixture of **4aH**$^+$ and **4bH**$^+$ (Figure 5). Our computational prediction is that any reference base with a PA greater than or equal to roughly 208 kcal/mol (the PA of the most basic site of **4a**) should be able to deprotonate **4aH**$^+$. Consistent with this prediction, we do observe proton transfer for all reference bases from 2′,4′-dimethylacetophenone (PA = 210.9 kcal/mol) to *n*-propylamine (PA = 219.4 kcal/mol) (Table 2, fourth column).

The "opposite" direction reaction is that of the protonated reference base with Apn (third column, Table 2). If both **4a** and **4b** are present, then the prediction is that we should see reaction for any protonated reference base with a PA of about 216 kcal/mol or less, because **4b** has a calculated PA of 216.4 kcal/mol (Figure 5). We do see proton transfer for all reference bases with PAs of 215.3 kcal/mol and lower. This points to the presence of **4b**, because if only **4a** was present, we would not see proton transfer for reference bases with PAs above about 208 kcal/mol.

The presence of both **4a** and **4b** is therefore consistent with the wide range of proton transfer in both directions that we see in Table 2. We thus believe that under our experimental conditions, we have a mixture of Apn tautomers **4a** and **4b**.

Briefly, in terms of acidity, both **4a** and **4b** have a calculated acidity of about 333 kcal/mol (Figure 5; also confirmed with M06-2X/6-31++G(2d,p) calculations, which yield a calculated acidity of 334 kcal/mol), so acidity cannot be used as a means of providing evidence for the presence of one tautomer versus the other. The measured values for the acidity of Apn are 335 ± 3 kcal/mol by Cooks' kinetic method and 337 ± 4 kcal/mol by bracketing. Although the bracketing value is not as close to the calculated value as that obtained by Cooks' kinetic method, both are in agreement with the computed acidity of 333 kcal/mol, within error.

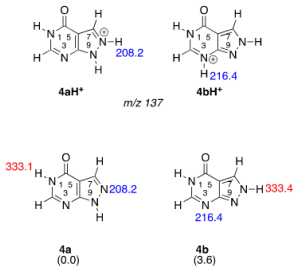

FIGURE 5 Structures of **4a**, **4b**, **4aH**$^+$, and **4bH**$^+$. Calculated proton affinities (the most basic sites) are shown in blue; calculated acidities (the most acidic sites) are shown in red. Relative stabilities of the two tautomers are shown in parentheses. Calculations were conducted at B3LYP/6-31+G(d) and reported as ΔH at 298 K, in kcal/mol

3.2 | Biological implications

The compounds studied herein are substrates for the enzyme, Hu HGPRT. Hu HGPRT catalyzes the conversion of purine nucleobases to nucleoside monophosphates through the transfer of a phosphoribosyl moiety (Scheme 1). HGPRT is a target for antiparasitic, particularly antimalarial development. Parasites are often wholly dependent on salvage pathways that utilize PRT enzymes, to synthesize DNA, whereas mammals have both the salvage and de novo DNA synthesis pathways.[7,14,21–24] Therefore, inhibiting the salvage pathway is a way to specifically target parasites.

The human HGPRT mechanism is not fully understood.[1,3,10,21–24,39–56] One point of interest is the timing of deprotonation of the N7–H proton; this deprotonation could be envisioned either before or after nucleophilic attack (Figure 6, shown for a general purine nucleobase).

In prior work, we have found that gas-phase properties often lend insight into enzyme mechanism, particularly in cases where the enzyme active sites provide a hydrophobic environment.[25–36] Experiments in the gas phase reveal intrinsic reactivity that can be correlated to the nonpolar interior of the enzyme. Enzymes that have a wide range of substrates, such as Hu HGPRT, often discriminate between various substrates by providing a hydrophobic environment, because differences in reactivity are often enhanced in such environments. Some HGPRTs are believed to have a key loop that protects the transition state from bulk solvent.[51,57] Our gas-phase experimental and calculational data can therefore potentially help reveal aspects of the Hu HGPRT mechanism.

In Mechanism 1 (Figure 6), deprotonation precedes substitution, such that the nucleophile would be the deprotonated nucleobase **6**. If **6** is the nucleophile, then a first pass to assess nucleophilicity would be to probe the basicity of the anion **6** at the N9 position (or the acidity of the conjugate acid **5a**, at N9–H). Should Mechanism 1 be operative, we would therefore expect the N9 basicity of anion **6** to correlate to the HGPRT phosphoribosylation rate for the various substrates. Table 5 shows the calculated N9–H acidities of **5a** (which

TABLE 5 HGPRT rate constants and basicity of N9 anion (structure **6**)

Substrate	k_{cat} (s^{-1})[a]	N9 anion basicity[b]
Guanine (G, **7**)	13.4	334.3[c]
6-Thioguanine (6-Tg, **1**)	7.6	328.4
Hypoxanthine (Hx, **8**)	7.4	330.5[d]
6-Mercaptopurine (6-Mp, **2**)	1.8	324.5
Allopurinol (Apn, **4**)	0.08	336.9
8-Azaguanine (8-Ag, **3**)	Not measurable	330.0

[a]At pH 8.5, from Keough et al.[24]
[b]Values calculated at B3LYP/6-31+G(d); all values are ΔH in kcal/mol.
[c]Zhachkina et al.[32]
[d]Sun and Lee.[26]

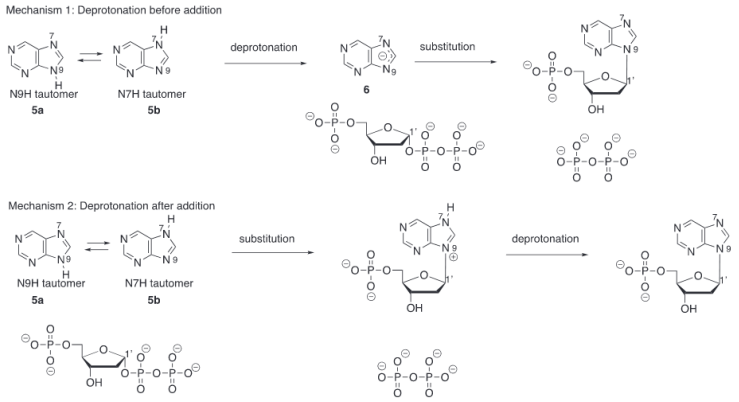

FIGURE 6 Possible mechanisms for the reaction catalyzed by human HGPRT, shown for a general purine nucleobase

corresponds to the basicity of **6** at N9) for the HGPRT substrates studied herein, as well as other known substrates for which there are experimental data (guanine and hypoxanthine, Figure 7, previously studied by our lab as well).[26,32,58] The rate of phosphoribosylation by HGPRT is also shown, and the substrates are ordered in decreasing k_{cat} values.

If the deprotonated anion **6** is the nucleophile, one would expect the N9 anion basicity (last column, Table 5) to steadily decrease as one moves down the table, because the entries are ordered in decreasing k_{cat}. However, the trends for N9 anion basicity and k_{cat} do not correlate. Although the k_{cat} values decrease in the order: G > 6-Tg > Hx > 6-Mp > Apn > 8-Ag, N9 anion basicity decreases as Apn > G > Hx > 8-Ag > 6-Tg > 6-Mp. These data imply that at least for our model, Mechanism 1 is not supported.

For Mechanism 2 (Figure 6), the neutral nucleobase is the nucleophile. For this mechanism, the N7H tautomer (**5b** in Figure 6) would be the most likely structure for the nucleophile, as the N9H tautomer **5a** has the proton on the N9 position, rendering it less nucleophilic. Prior studies over the years have identified an aspartate (Asp 137 in human HGPRT) that appears to stabilize the proton on the N7, favoring the N7H tautomer **5b**.[3,21,42,43,46,47,54,59] This aspartate is also believed to aid in the deprotonation step.

Regarding the N9H (**5a**) versus the N7H (**5b**) tautomer, the predominant tautomer by calculation is shown for each nucleobase in Table 6. We calculated each tautomer using B3LYP/6-31+G(d), M06-2X/6-311++G(2d,p), B3LYP/D3(BJ)/6-311++G(2d,p), ωb97X-D/6-311++G(2d,p), and DLPNO-CCSD(T)/aug-cc-pVTZ//M06-2X/6-311++G(2d,p). We also include guanine (**7**) and hypoxanthine (**8**), which are HGPRT substrates. Interestingly, we find that for the poor HGPRT substrates (those with lower k_{cat} values—Apn (**4**) and 8-Ag (**3**))—the most stable tautomer in the gas phase is the N9H tautomer **5a** (Table 6, third column). This is of interest, because for Mechanism 2, the N7H tautomer, *not the N9H* tautomer, is the desired structure. Apn (**4**), which has a slow phosphoribosylation rate, and 8-Ag (**3**), which is so slow that it is reported as not measurable, are both calculated, energetically, to prefer the unreactive N9H tautomer (**5a**) form in the gas phase. For the HGPRT substrates with larger k_{cat} values, guanine (**7**), hypoxanthine (**8**), and 6-Mp (**2**), the desired N7H tautomer is the most stable, and for 6-Tg (**1**), calculations indicate a mix, so the N7H form would still be present to react as a nucleophile. Thus, in a nonpolar site, the "best" substrates are already in the N7H tautomeric form (**5b**) that would favor nucleophilic attack. Our gas-phase results thus support a scenario where HGPRT provides a hydrophobic environment to "prime" certain nucleobases to nucleophilically attack PRPP, by favoring the nucleophilic tautomer N7H (**5b**).

If Mechanism 2 is operative, we would also expect the basicity of the neutral N7H tautomer, at the N9 position, to correlate to enzyme phosphoribosylation rates. Table 7 shows the k_{cat} versus the N9 PA for guanine, 6-Tg, hypoxanthine, and 6-Mp, the four substrates for HGPRT that have the fastest k_{cat} values. There is a correlation between

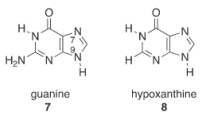

FIGURE 7 Structures of human HGPRT substrates guanine and hypoxanthine

TABLE 6 Most stable tautomer versus excision rates for Hu HGPRT substrates

Substrate	$k_{cat}(s^{-1})$[a]	Most stable tautomer, gas phase[b]
Guanine (**7**)	13.4	N7H[c] (**5b**)
6-Thioguanine (**1**)	7.6	N7H/N9H mix (**5a/5b**)
Hypoxanthine (**8**)	7.4	N7H[d] (**5b**)
6-Mercaptopurine (**2**)	1.8	N7H (**5b**)
Allopurinol (**4**)	0.08	N9H (**5a**)
8-Azaguanine (**3**)	NM	N9H (**5a**)

Abbreviation: NM, not measurable.
[a]At pH 8.5, from Keough et al.[24]
[b]Calculated at B3LYP/6-31+G(d), M06-2X/6-311++G(2d,p), B3LYP/D3(BJ)/6-311++G(2d,p), ωb97X-D/6-311++G(2d,p), and DLPNO-CCSD(T)//aug-cc-pVTZ//M06-2X/6-311++G(2d,p).
[c]Zhachkina et al.[32]
[d]Sun and Lee.[26]

TABLE 7 Human HGPRT rate constants and basicity of the most stable tautomer (N7H, **5b**)

Substrate	k_{cat} (s^{-1})[a]	N9 PA[b]
Guanine (**7**)	13.4	226.9[c]
6-Thioguanine (**1**)	7.6	225.3
Hypoxanthine (**8**)	7.4	218.8[d]
6-Mercaptopurine (**2**)	1.8	217.6

[a]At pH 8.5, from Keough et al.[24]
[b]Values calculated at B3LYP/6-31+G(d); all values are ΔH in kcal/mol.
[c]Zhachkina et al.[32]
[d]Sun and Lee.[26]

TABLE 8 Calculated $^{14}N/^{15}N$ (on N9) KIEs

Substrate	Mechanism 1	Mechanism 2
Guanine (**7**)	1.000	0.999
Hypoxanthine (**8**)	1.007	0.999

the rate of phosphoribosylation and the PA of the N9 position: Both the k_{cat} and the N9 PA decrease in the order of: G (**7**) > 6-Tg (**1**) > Hx (**8**) > 6-Mp (**2**). The intersection between the better substrates favoring the desired N7H tautomer in the gas phase, coupled with the in vacuo PA trend, lends support to a mechanism where nucleophilic attack precedes proton transfer (Mechanism 2).

3.3 | Kinetic isotope effects

Because isotope effects are so often useful for determining mechanism, we utilized calculations to ascertain whether heavy isotopes could potentially differentiate Mechanism 1 from Mechanism 2 (Figure 6).

We calculated the effect of substituting a heavy isotope for a normal isotope for various atoms (H, C, N, O, and P) in hypoxanthine and guanine, for both mechanisms. For Mechanism 1, the KIEs are calculated for ribosyl transfer with the deprotonated purine nucleobase (**6**). For Mechanism 2, the KIEs are calculated for ribosyl transfer with neutral purine nucleobase (**5b**). We found that substitution of the N9 with ^{15}N could potentially differentiate between the two mechanisms (Table 8). With guanine (**7**), the calculated KIE for Mechanism 1 is 1.000—the ^{15}N is not predicted to change the rate constant, relative to ^{14}N. The $^{14}N/^{15}N$ KIE for Mechanism 2, by contrast, is calculated to be slightly inverse (0.999). These KIEs are probably too similar to be used to differentiate mechanism. However, the contrast is more prominent for hypoxanthine (**8**). Mechanism 1 has a calculated normal $^{14}N/^{15}N$ KIE of 1.007, whereas for Mechanism 2, the KIE is inverse (0.999). Depending on the precision and accuracy of the experimental KIE, this difference might potentially be utilized to differentiate the two mechanisms.[60–62] Thus, an $^{14}N/^{15}N$ KIE could potentially be used to differentiate the two mechanisms (Figure 6). Such an experiment, if successful, would provide strong evidence supporting the nature of the nucleophilic purine nucleobase.

4 | CONCLUSIONS

We have calculated and measured, for the first time, the gas-phase thermochemical properties of four nucleobase substrates of HGPRT (6-Tg, 6-Mp, 8-Ag, and Apn). Specifically, we calculated the relative energies of the possible tautomers, and the acidities and PAs of the various acidic and basic sites on each purine tautomer. Comparison of our gas-phase experimental data with computations provides a valuable benchmark for the calculations. We also utilized the experiments and calculations to ascertain that under our experimental conditions, both the N9H and N8H tautomers of Apn are likely to be present. The four nucleobases, plus substrates hypoxanthine and guanine, are examined in the context of HGPRT. The thermochemical properties support a mechanism where nucleophilic attack precedes proton transfer. Furthermore, we propose that $^{14}N/^{15}N$ kinetic isotope effects could potentially be used to differentiate possible mechanisms.

5 | EXPERIMENTAL

All the experimentally measured substrates are commercially available and were used without further purification.

For Apn, acidity and PA values were bracketed using a Fourier transform ion cyclotron resonance mass spectrometer (FT-ICR or FTMS) with a dual cell setup, which has been described previously.[25,28,29,63,64] The magnetic field is 3.3 T, and the baseline pressure is 1×10^{-9} Torr. The Finnigan FTMS is equipped with a heated batch inlet system, a pulsed valve system, and a heatable solids probe. Apn was introduced into the system using the heatable solids probe. The reference acids and bases were introduced via a system of heatable batch inlets or leak valves. Water was pulsed into the cell via the pulsed valve system and ionized by an electron beam to generate either hydroxide (8 eV, 9 μA, and 0.5 s) or hydronium (20 eV, 6 μA, and 0.5 s) ions for acidity and PA measurements, respectively.

Acidity is the enthalpy of reaction for the transformation shown in Equation 1, and PA is the enthalpy of reaction for the transformation shown in Equation 2.

$$HA \rightarrow A^- + H^+ \quad (1)$$

$$B + H^+ \rightarrow BH^+ \quad (2)$$

We have previously described the typical protocol for measuring gas-phase reaction rate constants.[25,29,30,36,64] The reactions between the nucleobase and reference acids and bases were measured in both directions. For acidity, in one direction, the deprotonated Apn anions were generated by reaction of the Apn with the

hydroxide ions. The Apn anions were then transferred from one cubic cell to another via a 2 mm hole in the middle trapping plate. Transferred ions were cooled with pulsed argon gas. When the Ar gas is pulsed in, the pressure typically rises to 10^{-5} Torr. The reference acid is leaked into the second cell, and the reaction of the transferred deprotonated Apn ions with the reference acid can be examined. In the opposite direction, the conjugate bases of the reference acid were generated by reaction with hydroxide. These anions were then transferred to the second cell to react with neutral Apn. The same methodology is used for PA, except protonated ions are generated from neutral compounds by reaction with hydronium. Experiments were conducted at ambient temperature. These reactions are run under pseudo-first-order conditions; the neutral reactant is in excess relative to the reactant anions or cations. Because measurement of the pressure of the neutral compounds by the ion gauges is not always accurate, we instead "back out" the pressure of the neutral substrate from fast control reactions (described previously).[26,29,32,36,65,66]

We also measured gas-phase acidity and PA using Cooks' kinetic method.[67–70] For these studies, we utilized a quadrupole ion trap. Cooks' kinetic method is well known; briefly, for acidity, a proton-bound dimer was generated between a reference acid HA with a known acidity and the nucleobase HX (Equation 3).

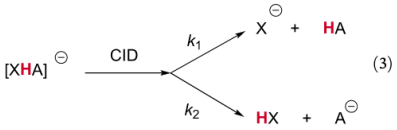

(3)

The proton-bound dimer was isolated, and then collision-induced dissociation (CID) was used to dissociate the complex into monomeric anions, either deprotonated nucleobase (via k_1) or deprotonated reference acid (via k_2). We can relate the rate constants (k_1 and k_2) to the acidity (ΔH_{acid}) of the nucleobases, as shown in Equation 4:

$$ln\left(\frac{k_1}{k_2}\right) \approx ln\left(\frac{[X^-]}{[A^-]}\right) = \frac{1}{RT_{eff}}(\Delta H_{acid}(HA) - \Delta H_{acid}(HX)) \quad (4)$$

where R is the gas constant and T_{eff} is the effective temperature (in Kelvin) of the activated complex.[71] The ratio of the abundances of the two deprotonated products yields the relative acidity of the two compounds of interest (Equation 4), assuming the dissociation has no energy barrier for the reverse reaction and that the dissociation transition structure is late and therefore indicative of the stability of the two deprotonated products.[72] These assumptions are generally true for proton-bound systems.[70,73,74] In order to obtain the acidity of compound HX, the natural logarithm of the relative abundance ratios is plotted versus the acidities for a series of reference acids, where the slope is $(1/RT_{eff})$ and the y intercept is $(-\Delta H_{acid}(HX)/RT_{eff})$. The T_{eff} is obtained from the slope. The acidity of the nucleobase, ΔH_{acid} (HX), can be calculated using Equation 4, or by using the y intercept $((-\Delta H_{acid}(HX)/RT_{eff})$. The plots for Cooks' kinetic method workup are in the supporting information.

Electrospray ionization (ESI), with an electrospray needle voltage of ~4.5 kV, was used to generate the proton-bound dimers from a solution with a concentration of 10^{-4} M, in methanol. The flow rate was 25 μl/min. The proton-bound dimer ions were isolated and then dissociated by applying CID; the complexes were activated for about 30 ms. Finally, the fragment product ions are detected to give the ratio of the deprotonated nucleobase and the deprotonated reference acid. A total of 40 scans were averaged for the product ions. The same method was used for PA measurements.

All DFT calculations were performed with Gaussian 16.[75] B3LYP[76–78] optimizations were performed using the 6-31+g(d) and 6-311++G(2d,p) basis sets,[79] with Grimme's dispersion correction D3 with Becke–Johnson dampening applied where noted.[80] ωB97X-D[81] and M06-2X[82,83] optimizations were performed using the 6-311++G(2d,p) basis set. All geometry optimizations were subjected to frequency calculations to verify stationary points as minima in the potential energy surface. Electronic energies were also calculated using the DLPNO-CCSD(T)[84] method with ORCA 4.2.1[85,86] from the M06-2X optimized structures. DLPNO-CCSD (T) calculations were performed using the aug-cc-pVTZ basis set.[87,88] For the isotope effects, frequency calculations were performed on the B3LYP/6-31+G (d) optimized geometries, and isotope effects were theoretically calculated using the Quiver program.[89–91]

ACKNOWLEDGMENT

We thank the National Science Foundation (NSF) for financial support.

DATA AVAILABILITY STATEMENT

Data are available upon request from the authors.

ORCID

Jeehiun K. Lee https://orcid.org/0000-0002-1665-1604

REFERENCES

[1] S. P. Craig III, A. E. Eakin, *J. Biol. Chem.* **2000**, *275*, 20231.
[2] W. D. L. Musick, *CRC Crit. Rev. Biochem.* **1981**, *11*, 1.
[3] J. C. Eads, G. Scapin, Y. Xu, C. Grubmeyer, J. C. Sacchettini, *Cell* **1994**, *78*, 325.
[4] M. Lesch, W. L. Nyhan, *Am. J. Med.* **1964**, *36*, 561.
[5] D. G. Sculley, P. A. Dawson, B. T. Emmerson, R. B. Gordon, *Hum. Genet.* **1992**, *90*, 195.
[6] B. L. Davidson, M. Pashmforoush, W. N. Kelley, T. D. Palella, *J. Biol. Chem.* **1989**, *264*, 520.
[7] A. King, D. W. Melton, *Nucleic Acids Res.* **1987**, *15*, 10469.
[8] S. P. Craig III, A. E. Eakin, *Parasitol. Today* **1997**, *13*, 238.
[9] P. J. Focia, S. P. Craig III, A. E. Eakin, *Biochemistry* **1998**, *37*, 17120.
[10] D. T. Keough, D. Hockova, A. Holy, L. M. Naesens, T. S. Skinner-Adams, J. de Jersey, L. W. Guddat, *J. Med. Chem.* **2009**, *52*, 4391.
[11] D. Hockova, D. T. Keough, Z. Janeba, T. H. Wang, J. de Jersey, L. W. Guddat, *J. Med. Chem.* **2012**, *55*, 6209.
[12] D. T. Keough, P. Spacek, D. Hockova, T. Tichy, S. Vrbkova, L. Slavetinska, Z. Janeba, L. Naesens, M. D. Edstein, M. Chavchich, T. H. Wang, J. de Jersey, L. W. Guddat, *J. Med. Chem.* **2013**, *56*, 2513.
[13] M. M. Kaiser, D. Hockova, T. H. Wang, M. Dracinsky, L. Postova-Slavetinska, E. Prochazkova, M. D. Edstein, M. Chavchich, D. T. Keough, L. W. Guddat, Z. Janeba, *ChemMedChem* **2015**, *10*, 1707.
[14] D. T. Keough, A.-L. Ng, D. J. Winzor, B. T. Emmerson, J. de Jersey, *Mol. Biochem. Parasitol.* **1999**, *98*, 29.
[15] M. H. el Kouni, *Pharmacol. Ther.* **2003**, *99*, 283.
[16] P. Gayathri, H. Balaram, M. R. Murthy, *Curr. Opin. Struct. Biol.* **2007**, *17*, 744.
[17] T. Cheviet, I. Lefebvre-Tournier, S. Wein, S. Peyrottes, *J. Med. Chem.* **2019**, *62*, 8365.
[18] D. L. Gardiner, T. S. Skinner-Adams, C. L. Brown, K. T. Andrews, C. M. Stack, J. S. McCarthy, J. P. Dalton, K. R. Trenholme, *Expert Rev. Anti-Infective Ther.* **2009**, *7*, 1087.
[19] P. Acharya, R. Pallavi, S. Chandran, H. Chakravarti, S. Middha, J. Acharya, S. Kochar, D. Kochar, A. Subudhi, A. P. Boopathi, S. Garg, A. Das, U. Tatu, *Proteomics Clin. Appl.* **2009**, *3*, 1314.
[20] J. de Jersey, A. Holy, D. Hockova, L. Naesens, D. T. Keough, L. W. Guddat, *Curr. Top. Med. Chem.* **2011**, *11*, 2085.
[21] V. Karnawat, S. Gogia, H. Balaram, M. Puranik, *ChemPhysChem* **2015**, *16*, 2172.
[22] T. A. Krenitsky, R. Papaioannou, G. B. Elion, *J. Biol. Chem.* **1969**, *244*, 1263.
[23] T. A. Krenitsky, R. Papaioannou, *J. Biol. Chem.* **1969**, *244*, 1271.
[24] D. T. Keough, T. S. Skinner-Adams, M. K. Jones, A.-L. Ng, I. M. Brereton, L. W. Guddat, J. de Jersey, *J. Med. Chem.* **2006**, *49*, 7479.
[25] M. Liu, M. Xu, J. K. Lee, *J. Org. Chem.* **2008**, *73*, 5907.
[26] X. Sun, J. K. Lee, *J. Org. Chem.* **2007**, *72*, 6548.
[27] J. K. Lee, *Int. J. Mass Spectrom.* **2005**, *240*, 261.
[28] S. Sharma, J. K. Lee, *J. Org. Chem.* **2002**, *67*, 8360.
[29] M. A. Kurinovich, J. K. Lee, *J. Am. Chem. Soc.* **2000**, *122*, 6258.
[30] M. A. Kurinovich, J. K. Lee, *J. Am. Soc. Mass Spectrom.* **2002**, *13*, 985.
[31] X. Sun, J. K. Lee, *J. Org. Chem.* **2010**, *75*, 1848.
[32] A. Zhachkina, M. Liu, X. Sun, F. S. Amegayibor, J. K. Lee, *J. Org. Chem.* **2009**, *74*, 7429.
[33] A. Z. Michelson, A. Rosenberg, Y. Tian, X. Sun, J. Davis, A. W. Francis, V. L. O'Shea, M. Halasyam, A. H. Manlove, S. S. David, J. K. Lee, *J. Am. Chem. Soc.* **2012**, *134*, 19839.
[34] A. Z. Michelson, M. Chen, K. Wang, J. K. Lee, *J. Am. Chem. Soc.* **2012**, *134*, 9622.
[35] G. S. M. Kiruba, J. Xu, V. Zelikson, J. K. Lee, *Chem. Eur. J.* **2016**, *22*, 3881.
[36] M. Liu, T. Li, F. S. Amegayibor, D. S. Cardoso, Y. Fu, J. K. Lee, *J. Org. Chem.* **2008**, *73*, 9283.
[37] P. J. Linstrom, W. G. Mallard, *NIST Chemistry WebBook, NIST Standard Reference Database Number 69*, National Institute of Standards and Technology, Gaithersburg, MD **2019**. http://webbook.nist.gov
[38] When **3a** is protonated at N9, the optimized structure is ring-opened, with no N8–N9 bond.
[39] A. Thomas, M. J. Field, *J. Am. Chem. Soc.* **2002**, *124*, 12432.
[40] A. Thomas, M. J. Field, *J. Am. Chem. Soc.* **2006**, *128*, 10096.
[41] Y. Xu, J. Eads, J. C. Sacchettini, C. Grubmeyer, *Biochemistry* **1997**, *36*, 3700.
[42] Y. Xu, C. Grubmeyer, *Biochemistry* **1998**, *37*, 4114.
[43] V. L. Schramm, C. Grubmeyer, *Prog. Nucleic Acid Res. Mol. Biol.* **2004**, *78*, 261.
[44] P. Gayathri, S. Subbayya, C. S. Ashok, T. S. Sevli, H. Balaram, M. R. N. Murthy, *Proteins Struct. Funct. Genet.* **2008**, *73*, 1010.
[45] S. Gogia, H. Balaram, *M. Puranik* **2011**, *50*, 4184.
[46] C. M. Li, P. C. Tyler, R. H. Furneaux, G. Kicska, Y. Xu, C. Grubmeyer, M. E. Girvin, V. L. Schramm, *Nat. Struct. Biol.* **1999**, 582.
[47] W. Shi, C. M. Li, P. C. Tyler, R. H. Furneaux, C. Grubmeyer, V. L. Schramm, S. C. Almo, *Nat. Struct. Biol.* **1999**, *6*, 588.
[48] V. L. Schramm, W. Shi, *Curr. Opin. Struct. Biol.* **2001**, *11*, 657.
[49] R. G. Ducati, R. S. Firestone, V. L. Schramm, *Biochemistry* **2017**, *56*, 6368.
[50] S. C. Sinha, J. L. Smith, *Curr. Opin. Struct. Biol.* **2001**, *11*, 733.
[51] A. Jardim, B. Ullman, *J. Biol. Chem.* **1997**, *272*, 8967.
[52] A. Heroux, E. L. White, L. J. Ross, D. W. Borhani, *Biochemistry* **1999**, *38*, 14485.
[53] A. Heroux, E. L. White, L. J. Ross, R. L. Davis, D. W. Borhani, *Biochemistry* **1999**, *38*, 14495.
[54] B. Canyuk, P. J. Focia, A. E. Eakin, *Biochemistry* **2001**, *40*, 2754.
[55] R. K. Goitein, D. Chelsky, S. M. Parsons, *J. Biol. Chem.* **1978**, *253*, 2963.
[56] G. K. Balendiran, J. A. Molina, Y. Xu, J. Torres-Martinez, R. C. Stevens, P. J. Focia, A. E. Eakin, J. C. Sacchettini, S. P. Craig III, *Protein Sci.* **1999**, *8*, 1023.
[57] M. Schumacher, D. Carter, D. S. Roos, B. Ullman, R. G. Brennan, *Nat. Struct. Biol.* **1996**, *3*, 881.
[58] Note that when deprotonated, both the N9H (**5a**) and N7H tautomers (**5b**) yield the same anion (**6**). Therefore, the acidity at the N9–H is the relevant value, even if the N9H tautomer is not the most stable.
[59] W. Shi, C. M. Li, P. C. Tyler, R. H. Furneaux, S. M. Cahill, M. E. Girvin, C. Grubmeyer, V. L. Schramm, S. C. Almo, *Biochemistry* **1999**, *38*, 9872.

[60] D. A. Singleton, A. A. Thomas, *J. Am. Chem. Soc.* **1995**, *117*, 9357.
[61] D. A. Singleton, S. A. Merrigan, B. J. Kim, P. Beak, L. M. Phillips, J. K. Lee, *J. Am. Chem. Soc.* **2000**, *122*, 3296.
[62] K.-Y. Kuan, D. A. Singleton, *J. Org. Chem.* **2021**, *86*, 6305.
[63] S. Sharma, J. K. Lee, *J. Org. Chem.* **2004**, *69*, 7018.
[64] M. A. Kurinovich, L. M. Phillips, S. Sharma, J. K. Lee, *Chem. Commun.* **2002**, 2354.
[65] W. J. Chesnavich, T. Su, M. T. Bowers, *J. Chem. Phys.* **1980**, *72*, 2641.
[66] T. Su, W. J. Chesnavich, *J. Chem. Phys.* **1982**, *76*, 5183.
[67] R. G. Cooks, T. L. Kruger, *J. Am. Chem. Soc.* **1977**, *99*, 1279.
[68] S. A. McLuckey, D. Cameron, R. G. Cooks, *J. Am. Chem. Soc.* **1981**, *103*, 1313.
[69] S. A. McLuckey, R. G. Cooks, J. E. Fulford, *Int. J Mass Spectrom Ion Phys.* **1983**, *52*, 165.
[70] K. B. Green-Church, P. A. Limbach, *J. Am. Soc. Mass Spectrom.* **2000**, *11*, 24.
[71] L. Drahos, K. Vekey, *J. Mass Spectrom.* **1999**, *34*, 79.
[72] R. G. Cooks, J. S. Patrick, T. Kotiaho, S. A. McLuckey, *Mass Spectrom. Rev.* **1995**, *13*, 287.
[73] K. M. Ervin, *Chem. Rev.* **2001**, *101*, 391.
[74] S. Gronert, W. Y. Feng, F. Chew, W. Wu, *Int. J. Mass Spectrom.* **2000**, *196*, 251.
[75] M. J. Frisch, G. W. Trucks, H. B. Schlegel, G. E. Scuseria, M. A. Robb, J. R. Cheeseman, G. Scalmani, V. Barone, G. A. Petersson, H. Nakatsuji, X. Li, M. Caricato, A. V. Marenich, J. Bloino, B. G. Janesko, R. Gomperts, B. Mennucci, H. P. Hratchian, J. V. Ortiz, A. F. Izmaylov, J. L. Sonnenberg, D. Williams-Young, F. Ding, F. Lipparini, F. Egidi, J. Goings, B. Peng, A. Petrone, T. Henderson, D. Ranasinghe, V. G. Zakrzewski, J. Gao, N. Rega, G. Zheng, W. Liang, M. Hada, M. Ehara, K. Toyota, R. Fukuda, J. Hasegawa, M. Ishida, T. Nakajima, Y. Honda, O. Kitao, H. Nakai, T. Vreven, K. Throssell, J. A. Montgomery Jr., J. E. Peralta, F. Ogliaro, M. J. Bearpark, J. J. Heyd, E. N. Brothers, K. N. Kudin, V. N. Staroverov, T. A. Keith, R. Kobayashi, J. Normand, K. Raghavachari, A. P. Rendell, J. C. Burant, S. S. Iyengar, J. Tomasi, M. Cossi, J. M. Millam, M. Klene, C. Adamo, R. Cammi, J. W. Ochterski, R. L. Martin, K. Morokuma, O. Farkas, J. B. Foresman, D. J. Fox, *Gaussian 16, Revision B.01*, Gaussian, Inc., Wallingford, CT **2016**.
[76] A. D. Becke, *J. Chem. Phys.* **1993**, *98*, 5648.
[77] C. Lee, W. Yang, R. G. Parr, *Phys. Rev. B* **1988**, *37*, 785.
[78] A. D. Becke, *J. Chem. Phys.* **1993**, *98*, 1372.
[79] W. Kohn, A. D. Becke, R. G. Parr, *J. Phys. Chem.* **1996**, *100*, 12974.
[80] S. Grimme, S. Ehrlich, L. Goerigk, *J. Comput. Chem.* **2011**, *32*, 1456.
[81] J.-D. Chai, M. Head-Gordon, *Phys. Chem. Chem. Phys.* **2008**, *10*, 6615.
[82] Y. Zhao, D. G. Truhlar, *Theor. Chem. Accounts* **2008**, *120*, 215.
[83] Y. Zhao, D. G. Truhlar, *Acc. Chem. Res.* **2008**, *41*, 157.
[84] Y. Guo, C. Riplinger, U. Becker, D. G. Liakos, Y. Minenkov, L. Cavallo, F. Neese, *J. Chem. Phys.* **2018**, *148*, 011101.
[85] F. Neese, *Wiley Interdisciplinary Reviews – Comp. Molec. Sci.* **2012**, *2*, 73.
[86] F. Neese, F. Wennmohs, U. Becker, C. Riplinger, *J. Chem. Phys.* **2020**, *152*, 224108.
[87] R. A. Kendall, T. H. Dunning Jr., R. J. Harrison, *J. Chem. Phys.* **1992**, *96*, 6796.
[88] D. E. Woon, T. H. Dunning Jr., *J. Chem. Phys.* **1993**, *98*, 1358.
[89] J. Bigeleisen, M. G. Mayer, *J. Chem. Phys.* **1947**, *15*, 261.
[90] M. Wolfsberg, *Acc. Chem. Res.* **1972**, *5*, 225.
[91] M. Saunders, K. E. Laidig, M. Wolfsberg, *J. Am. Chem. Soc.* **1989**, *111*, 8989.

SUPPORTING INFORMATION

Additional supporting information may be found in the online version of the article at the publisher's website.

How to cite this article: L. Zhang, D. J. Hinz, G. S. M. Kiruba, X. Ding, J. K. Lee, *J Phys Org Chem* **2022**, e4343. https://doi.org/10.1002/poc.4343